Experimental investigation of the spin reorientation of Co/Au based magnetic nanodot arrays

L. Gridneva,[1,*] A. Persson,[1] M. Á. Niño,[2,†] J. Camarero,[2] J. J. de Miguel,[2] R. Miranda,[2,3] C. Hofer,[4] C. Teichert,[4] T. Bobek,[5] A. Locatelli,[6] S. Heun,[7] S. Carlsson,[8] and D. Arvanitis[1]

[1]*Department of Physics, Uppsala University, Box 530, S-75121 Uppsala, Sweden*

[2]*Departamento de Física de la Materia Condensada and Instituto de Física de Materiales "Nicolás Cabrera," Universidad Autónoma de Madrid, Cantoblanco, 28049 Madrid, Spain*

[3]*Instituto Madrileño de Estudios Avanzados en Nanociencia (IMDEA Nanociencia), Cantoblanco, 28049-Madrid, Spain*

[4]*Institut für Physik, Montanuniversität Leoben, Franz Josef Strasse 18, A-8700 Leoben, Austria*

[5]*Institute of Semiconductor Electronics, Aachen University, Sommerfeldstrasse 24, 52074 Aachen, Germany*

[6]*Sincrotrone Trieste, S.S. 14, km 163.5, 34012 Basovizza, Trieste, Italy*

[7]*NEST CNR-INFM Scuola Normale Superiore, Piazza dei Cavalieri 7, 56126 Pisa, Italy*

[8]*MAX-lab, Box 118, S-22100, Lund, Sweden*

(Received 27 June 2007; revised manuscript received 1 November 2007; published 19 March 2008)

(Co/Au) and (Au/Co/Au) nanomagnet arrays grown on nanostructured self-organized SiGe templates have been characterized by means of x-ray photoemission electron microscopy, x-ray magnetic circular dichroism, and by extended x-ray absorption spectroscopy using synchrotron radiation. In-plane magnetization is observed at room temperature for practically all Co thicknesses, a stable macroscopic perpendicular magnetic order only at low temperature. The spin reorientation transition in these dot arrays takes place for smaller Co thicknesses over a broader thickness range than in two-dimensional systems. This finding appears to be related with structural relaxation modifications, occurring within the local Co atom environment, which are not necessarily connected with the orbital moment variations. These variations appear in the form of a systematic increase, correlated with the existence of out-of-plane magnetization.

DOI: 10.1103/PhysRevB.77.104425 PACS number(s): 75.75.+a, 78.70.Dm, 75.70.Rf

I. INTRODUCTION

At the present rate of advance in the process of miniaturization of the bit sizes in magnetic storage media, which even surpasses the famous Moore's law for semiconductor devices,[1] storage densities of the order of Tb/cm^{-2} are about to be reached in the near future.[2] At such densities the size of the individual bits must be of the order of a few nanometers, a range in which the magnetic characteristics of bulk materials change substantially. Hence, the characterization and understanding of the magnetization processes in those nanostructured materials becomes essential.

One of the main problems faced when reducing the volume of the individual magnetic bits is the appearance of the superparamagnetic effect, that is, the tendency of the object's magnetic moment to change direction due to the increased influence of thermal fluctuations. Different strategies have been proposed to overcome this limitation,[3] but the most promising one relies on switching the magnetization direction from in plane, as is commonly used nowadays, to out of plane. This would facilitate higher storage densities[4] by increasing the materials' magnetic anisotropy (and hence the thermal stability of their magnetic moments) and it would also improve the signal-to-noise ratio in readout due to the better alignment of the bits magnetization with the reading head.[5] The directions of the easy axes of magnetization result from interplay between different energetic contributions: while the interfacial anisotropy favors out-of-plane orientation,[6] the shape term usually tends to rotate the magnetization into the surface plane. In general, the magnetic anisotropy is a subtle effect derived from spin-orbit coupling and it is therefore very sensitive to even the minor details of the electronic structure and the local atomic environment of the material under investigation. The strategy to continue increasing the storage density also involves substituting the currently used continuous media, in which a bit is formed by hundreds of grains, by discrete ones where a bit of information is stored in a single particle, separated from the rest. In this way, the need for averaging would be suppressed and the noise caused by the deviations in the signal produced by each grain could be greatly reduced.[2] Most of the approaches undertaken so far along this line have been based on nanolithography methods to define the desired structures on the appropriate medium. This approach offers the highest degree of control over the nanostructures sizes, shapes, and arrangement, but on the other hand its processing time, technical complexity, and, hence, economic cost increase exponentially with any further step of miniaturization.

These facts have prompted the search for other, more efficient alternatives. A very suggestive approach, featuring both high production speed and low cost, although at the expense of more difficult control over the nanostructures' characteristics and uniformity, relies on the phenomenon of self-organization.[7] In recent years several promising methods for creating ordered arrays of magnetically independent nanodots based on self-organization have been developed.[8,9] In particular, the fabrication of patterned media by UHV grazing incidence deposition on spontaneously structured SiGe substrates has demonstrated a potential for parallel mass production of structures reaching lateral sizes as small as 25 nm with good long-range periodicity.[10,11] In arrays of magnetically decoupled nanodots, the reduced dimensionality of the objects further facilitates the destabilization of their magnetization by thermal fluctuations, as compared to continuous, two-dimensional thin films. Materials with high magnetic an-

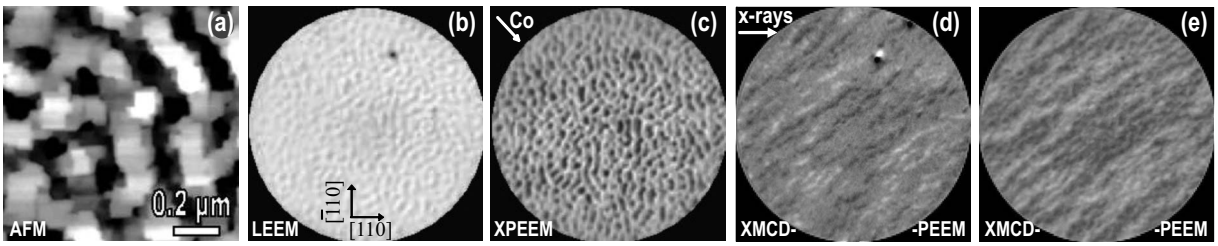

FIG. 1. (a) 1 μm$\times$1 μm AFM image of a self-organized $Si_{0.5}Ge_{0.5}$ surface consisting of {113}-faceted pyramids with (001) top surface; gray scale range: 20 nm. (b) LEEM image of a self-organized $Si_{0.5}Ge_{0.5}$ template after covering it with a 25 ML buffer of Au. (c) and (d) XPEEM and XMCD-PEEM images of the same sample after deposition of 3 ML (approximately 6 Å) Co at grazing incidence onto the Au/SiGe template. (e) XMCD-PEEM image of a 6-ML-thick Co film on the same substrate. All images were measured at room temperature. The field of view is 10 μm in images (b)–(e). For images (c)–(e), the photon energy was tuned to the Co L_3 edge (778 eV) and circularly polarized light was used. Polar angles of both the Co beam and the x rays with respect to the sample plane were 16°. Their projections to the sample plane are the same for all the experiments and are shown in (c) and (d). The crystallographic directions are shown in (b) for all the experiments.

isotropy energy need then to be used in order to stabilize a remanent magnetization at relatively high temperatures. For this purpose, we have chosen the well-known (Co/Au) system.[12] Multilayer stacks of alternating magnetic or nonmagnetic metal layers have been exploited to induce a perpendicular alignment of the magnetization by taking advantage of the accumulation of interfaces. This effect would be reinforced by the use of Au, which introduces a strong spin-orbit scattering of the electronic states at the Fermi level and thus provides a unique possibility to tailor the magnetic anisotropy of the dots. Nevertheless, the translation of these concepts from an infinite, two-dimensional system to a quasi-zero-dimensional one seems far from evident. Many properties are known to change substantially when the materials' dimensions are reduced: for instance, the magnetization reversal mechanism may change from domain nucleation and growth to coherent rotation.[13] Also the spin excitation and the magnetic normal mode are different.[14] Furthermore, novel crystal phases may be stabilized which are not generally preferred in bulk samples. In particular, the predominance of surface and interface effects in nanometric dots can give rise to anomalous relaxations and changes in the nearest neighbor distances that strongly affect magnitudes such as spin-orbit coupling or magnetic anisotropy. It is therefore necessary to carefully explore the characteristics of these novel types of materials.

In this paper we report on the study of the spin reorientation for *in situ* prepared (Au/Co/Au) dots on SiGe at both room temperature and 100 K using spectromicroscopy and x-ray magnetic circular dichroism (XMCD) methods. We have been able to stabilize an out-of-plane macroscopic remanence only at 100 K while stable macroscopic in-plane remanence could be detected at the temperatures of 100 and 300 K. These results reveal that, with respect to the previous study with pure Co[11] by adding Au we have been able to introduce an enhanced magnetic anisotropy in the dots capable of stabilizing an out-of-plane magnetization at 100 K. At the same time we find an anomalous behavior of the magnetic orbital moments through the spin reorientation transition. This anomaly could be related to the dot formation. The extended x-ray absorption fine structure (EXAFS) measurements made at the Co *K* edge on the (Au/Co/Au) dots show that the spin reorientation transition is correlated with the structural changes of the Co lattice in the dots.

II. EXPERIMENT

In order to produce the arrays of magnetic dots, a self-organized, $Si_{0.5}Ge_{0.5}$ thin film[9,15] grown by molecular beam epitaxy and capped with 3 nm Si was used as a template. The surface consists of isotropically arranged, {113}-faceted pyramids terminated by a (001) top surface, which was characterized by atomic force microscopy (AFM), as shown in Fig. 1(a). Due to the lateral size of the base length of about 200 nm the features are well suited for the detection of independent magnetic areas by x-ray photoemission electron microscopy (XPEEM)-XMCD and the {113} facets, which are tilted 25.3° with respect to the surface, are advantageous to generate isolated nanomagnets, with no magnetic material in between, by shadow deposition.

(Au/Co/Au) stacks were grown by electron beam evaporation, with the base pressure in the 10^{-10} Torr range; Au was deposited at room temperature under normal incidence to cover the substrate more efficiently, whereas Co was evaporated at grazing incidence (16 degrees), taking advantage of the surface pattern relief to selectively cover determined areas while avoiding others ("*shadow effect*") as previously described.[11] In this way, the metallic film spontaneously arranges itself into aggregates distributed as dictated by the surface template. The samples were then studied as a function of Co and Au cap thickness.

A detailed understanding of the complex phenomena behind the magnetic anisotropy demands a very sensitive, element-specific probe of the local electronic structure, such as x-ray absorption spectroscopy (XAS). Furthermore, with the development of synchrotron radiation sources x-ray magnetic circular dichroism (XMCD), a technique based on XAS, has emerged as a powerful tool for the study of magnetism, allowing for a separate determination of the spin and orbital magnetic moments on a per-atom basis in ferromagnetic and antiferromagnetic systems.[16] The XAS process for 3*d* transition metals involves transitions from localized 2*p* core levels to the 3*d* states above the Fermi level with the same symmetry. The dipole selection rules ensure that the 2*p*

core levels are excited into the unoccupied 3*d* levels, here the states driving the magnetism.[16] Analysis of the spectral areas obtained by XMCD using magneto-optic sum rules yield the spin (m_S) and orbital (m_L) moments.[16] XMCD can provide the orbital moment anisotropy, which is related to the magnetic anisotropy energy, via *ab initio* theory calculations or even via a simple perturbation model approach.[17]

The XMCD signal is proportional to $\boldsymbol{k}\cdot\boldsymbol{M}$, where $\boldsymbol{k}$ is the radiation wave vector and $\boldsymbol{M}$ is the sample magnetization. Therefore, only the projection of the magnetization along the direction of the $\boldsymbol{k}$ vector is detected. This implies that for the experiments performed under normal x-ray incidence only the out-of-plane component of the magnetization is probed. Conversely, in the measurements carried out with the x rays impinging on the sample under grazing incidence, mainly the in-plane component of the magnetization is detected. The obtained magnetic moment values were corrected taking this fact into account, and also for the finite degree of helicity of the x rays.

Finally, it must be kept in mind that by measuring in remanence a reduced magnetization can be detected as compared to the saturation value. For an oblique x-ray incidence the XMCD signal has two contributions, one proportional to the in-plane magnetization and the other one proportional to the out-of-plane magnetization. To separate the perpendicular from the longitudinal components of the magnetization we apply the following procedure. To obtain the in-plane XMCD signal two sets of absorption spectra were recorded. First a magnetic field pulse of 650 G was applied in the horizontal plane, along the sample surface. The absorption spectrum was then recorded in remanence at an x-ray incidence of 45°, to get a sizable in-plane magnetization projection but to avoid saturation effects in total electron yield [see the inset of Fig. 2(b)]. Then, another pulse of magnetic field with opposite polarity was applied and the corresponding absorption spectrum was recorded, keeping the same photon helicity. For out-of-plane XMCD measurements both the incident x-ray beam and the applied pulses of the magnetic field of both polarities were perpendicular to the sample surface [inset of Fig. 2(a)]. After magnetizing the sample either in- or out-of-plane, the full polar angular dependence of the magnetization in the remanent state was measured: the angle of incidence of the x-ray beam was varied to determine the easy axes of magnetization. In this way it was observed that remanence could only be detected either in plane or out of plane, according to the applied magnetic field, but never along any intermediate direction. From the absorption spectra measured with opposite magnetizations the XMCD dichroic difference was calculated at both the L_3 and L_2 edges of Co. For the evaluation of the signal, the well-established sum rule procedure was used yielding the magnetization value per atom; the number of empty 3*d* states was set to 2.8.

The sample was characterized through XAS measurements at the C and O *K* edges. The thicknesses of both Co and Au were determined and cross-checked by means of a quartz crystal microbalance and by the change of the Co XAS signal-to-background ratio in the high energy continuum region of the spectra known as the "edge-jump ratio."[18] For low Co coverage the Co edge jump ratio is proportional to the amount of deposited material.[18] The Au

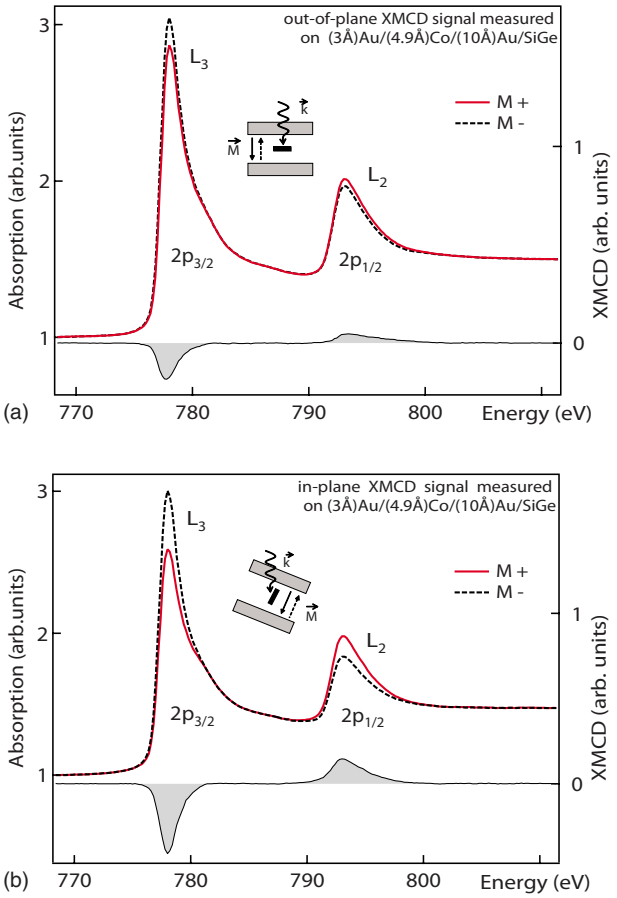

FIG. 2. (Color online) (a) Out-of-plane and (b) in-plane normalized XMCD absorption spectra (left-hand vertical axes) and XMCD difference (right-hand axes) measured at the Co L_3 and L_2 edges with circularly polarized light on a magnetized (3 Å)Au/(4.9 Å)Co/(10 Å)Au trilayer grown under UHV on a self-organized $Si_{0.5}Ge_{0.5}$ substrate template. The data are taken at 100 K. The insets show the experiment geometry employed for both measurements. As can be seen in the inset (a), only the out-of-plane component of the remanent magnetization could be found at normal incidence.

deposition was monitored through the exponential decrease of the Ge and Co edge-jump ratio as a function of Au thickness, using an electron escape depth of 1.7 nm. The XMCD spectroscopy measurements in x-ray absorption were performed at the magnetism dedicated UHV experimental station of the bending magnet-based beam line D1011 at MAX-lab.[19] The ability for independent polar rotation of both the sample and the coils creating the applied magnetic field, together with the possibility for *in situ* evaporation, make this setup optimal for vector magnetometry experiments. The degree of circular polarization of the x-ray photons was fixed at 75% during the dichroism experiments, offering the best compromise between the signal-to-noise ratio and long-term x-ray beam stability.[20] All the spectra were recorded in the remanent state using the photocurrent from the sample. The measurements were performed at temperatures of 300 and 100 K by cooling the sample with liquid nitrogen after evaporation. The size of the x-ray beam at the sample position is about 1 mm^2, so that the measured mag-

netic signal is averaged within it. In spite of the small thicknesses employed, relatively high edge-jump ratios ranging from 0.15 to 0.18 could be measured, which is sufficient for XMCD signal analysis.[21] The data were compared with reference samples to determine the degree of circular polarization—a thick Co film on Cu(111) and SiO_2 characterized *in situ*.

Hard x-ray XANES and EXAFS experiments were performed at beam line I811 of MAX-lab[22] on the same (Au/Co/Au) sample studied previously by XMCD. The beam was focused, collimated and cut to 1×1 mm^2. EXAFS spectra were measured at room temperature over the Co *K* edge in fluorescence yield mode. To maximize the signal-to-background ratio from the weak *K*-alpha fluorescence intensity from the dots, and in order to obtain good statistics at high *k* values we acquired the fluorescence signal at angles close to grazing incidence with long accumulation times. In order to prevent substrate Bragg reflections appearing in the EXAFS energy range, specific angles were chosen. The EXAFS spectra were analyzed using the "Athena" and "Artemis" codes.[23]

In this manuscript we refer to layer thickness in terms of interlayer thickness. To calculate the correspondence between the deposited monolayers and layers thickness in angstroms along the surface normal, the bulk lattice parameters for Co and Au can be used for a good approximation. This is justified by our EXAFS analysis which indicates a nonpseudomorphic Co growth and bulklike Co-Co distances as discussed in Sec. III B.

Photoemission electron microscopy experiments with x-ray magnetic circular dichroism (XMCD-PEEM) were carried out at the nanospectroscopy beam line of the synchrotron laboratory Elettra, in Trieste (Italy), following the same procedure as described elsewhere.[11] XPEEM measurements were performed with the photon energy tuned to the L_3 Co absorption edge, 778 eV. The XMCD-PEEM micrographs are obtained by subtracting two absorption images acquired at the same place on the surface with circularly polarized light of opposite helicities, and the experimental geometry imposes a 16° grazing incidence for the x-ray beam with respect to the surface. The samples were grown *in situ* by evaporation under similar geometrical conditions as those described above. Both deposition and imaging were conducted at room temperature.

III. RESULTS

A. Co *L* edge XMCD

Figures 1(b)–1(e) display the results of XMCD-PEEM measurements demonstrating that it is possible to fabricate and image arrays of Co/Au/SiGe nanomagnets exhibiting a macroscopic remanence at room temperature, with dimensions as small as 200×110 nm^2. A SiGe surface with truncated pyramidal islands was covered *ex situ* with a 25 ML (50 Å, assuming bulk lattice constants) buffer layer of Au by evaporation in a separate ultrahigh vacuum system. It was then transferred into the PEEM chamber, where it was used as a template for the deposition of the magnetic material. No carbon or oxygen contaminants could be detected by the XPS and XAS measurements made on the Au/SiGe templates.

The low energy electron microscopy (LEEM) image in Fig. 1(b) is sensitive to the topographic features and reveals the surface morphology. On top of this substrate template, Co was evaporated *in situ* step by step and imaged subsequently. The XPEEM image in Fig. 1(c) clearly shows that Co-rich regions follow the surface relief pattern. As the experimental geometry for the XPEEM measurements imposes a 16° grazing incidence for the x-ray beam the contrast observed in the XMCD-PEEM micrographs in Figs. 1(d) and 1(e) is associated mostly to the in-plane component of the surface magnetization. The "black" and "white" spots in the images hence correspond to an antiparallel or parallel alignment of the magnetization component in the direction of the x-ray wave vector in the surface plane, respectively. The excellent correspondence in average size, shape, and separation between the features observed in all those images demonstrates that the distribution of Co on the surface follows indeed the template dictated by the substrate pattern. The XMCD-PEEM measurements made in remanence on these samples reveal two important facts: first, that the Co nanoislands are ferromagnetic at room temperature, and second, that the orientations of their magnetizations are not independent from each other. Due to their small dimensions and short separations, in-plane magnetized nanomagnets are coupled by the magnetostatic interaction forming micrometer-sized domains each one comprising only a few dots.

The observation of in-plane magnetization in these samples is surprising: for thin films, literature reports a rather strong out-of-plane magnetism for 3.5 ML of Co on Au.[12] In fact, in the XMCD-PEEM image of Fig. 1(d) there exist many "gray" areas which show no magnetic contrast under the particular experimental conditions employed in these measurements. As will be discussed later, those areas are most likely out-of-plane magnetized. With further Co deposition the number of in-plane magnetized particles increases, in good agreement with the expectation that shape anisotropy gradually overcomes the interfacial contribution. The average domain size also becomes larger with increasing Co coverage, indicating that the dipolar coupling is becoming more effective. The assignment of perpendicular magnetization to the gray areas in the XMCD-PEEM images of Fig. 1 is supported by the observed spin reorientation transition, and it can also be cross-checked by means of XMCD vector magnetometry.

Figure 2 shows some characteristic XMCD spectra at the Co L_3 and L_2 absorption edges, measured at 100 K and at different polar angles on a (Au/Co/Au) trilayer grown at 300 K on the SiGe substrate. Together with the two XMCD spectra obtained for opposite directions of the sample magnetization, the dichroic difference is also depicted in each case. The XMCD difference displayed in Fig. 2(a) demonstrates that there exists a stable *out-of-plane* remanent magnetization at that temperature. Nevertheless, for the same sample a strong *in-plane* magnetization can also be observed, in good agreement with the magnetic configuration revealed by the XMCD-PEEM results of Fig. 1. All in all, this is the first report of out-of-plane remanence for individual (Co/Au)

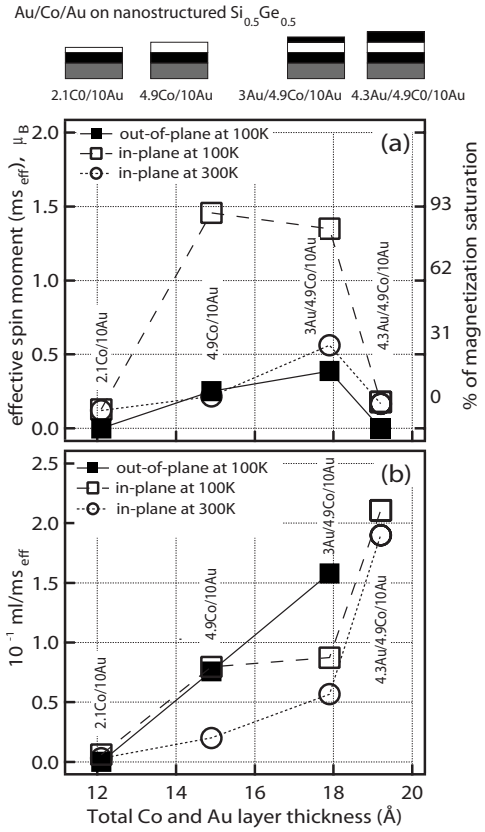

FIG. 3. Values of (a) the spin moment and (b) the orbital-to-spin moment ratio, derived from XMCD measurements performed at remanence on different (Co/Au) and (Au/Co/Au) structures grown on self-organized $Si_{0.5}Ge_{0.5}$ substrates. Squares (circles) correspond to data measured at 100 K (300 K). Filled and open symbols are for out-of-plane and in-plane magnetic moments, respectively. All the Co and Au thicknesses are given in angstroms.

dots over a macroscopic sample area, allowing, in particular, for a determination of the orbital part of the magnetic moment.

This information has been obtained from a detailed analysis of the XMCD data; an overview of the most relevant results is given in Fig. 3 as a function of the Co and the capping Au layer thicknesses. Both the in- and out-of-plane remanent magnetization can be analyzed using the magneto-optic sum rules yielding the spin and orbital moments separately, in μ_B per Co atom. Due to the averaging related to dot formation, the dipolar correction term (T_z) is expected to be small. The previous studies of two atomic layers, 8 nm diameter Co islands grown on Au(111) suggest the effective spin magnetic moment to be anisotropic and introduce a thickness-independent dipolar correction term T_z equal to $0.04\mu_B$ for the out-of-plane direction of magnetization and $-0.02\mu_B$ for the in-plane one.[24] In the case of the (Co/Au) dots under study here, the out-of-plane magnetic moment is isotropic and lower than that reported for the smaller Co islands (around $2\mu_B$ per Co atom). This observation, the fact that our (Co/Au) dots are much larger, and our EXAFS studies (see below) suggest that in this case Co atoms have a different local environment. Thus, based on the fact that we measure on an array of dots, the value of the spin moment is not corrected for the dipole term contributions. We still refer to an effective spin moment to avoid confusion even if this value should be rather close to the real one. Figures 3(a) and 3(b) present the dependence of both the effective spin moment and the ratio of the orbital-to-effective spin moment with Co and Au layer thicknesses. Solid (open) symbols indicate the values of out-of-plane (in-plane) moments; the open circles refer to in-plane moments measured at 300 K. No out-of-plane signal could be detected at that temperature.

As can be seen from Fig. 3 the deposition of Co and Au influences differently the effective value of the spin moment and the ratio of orbital-to-spin moment in remanence. Both the spin and the orbital moment scale to the amount of remanent magnetization, therefore the orbital-to-spin moment is independent from it.

Let us discuss first the behavior of the effective spin moment. The stable remanence increases steeply with Co deposition onto the Au buffer layer, both at 100 and 300 K. When the Co layer thickness reaches 4.9 Å the effective in-plane spin moment nearly reaches 100% of the corresponding Co reference standard value of $1.6\mu_B$ [see Fig. 3(a), right-hand vertical axis]. The out-of-plane component, in turn, reaches only about 10% of the full possible remanence, expected from previous results for Co/Au thin films and multilayers given in the literature.[12] The predominance of in-plane magnetization at the expense of the perpendicular alignment seen at Fig. 3(a) can result from magnetostatic coupling between the dots. In this case the magnetocrystalline anisotropy energy associated with the orbital moment anisotropy counteracts the magnetostatic interaction that favors an in-plane magnetization.[25]

In another study, combining theory and experiment,[26,27] it is shown that the proportionality between the magnetocrystalline anisotropy and the orbital moment anisotropy[17] breaks down, due to the strong *d-d* hybridization of the Co with the Au ligand atoms influenced by the large spin-orbit interaction with the Au atoms. Following these theoretical results, it may appear as a surprise that for uncapped (4.9 Å)Co/(10 Å)Au dots, the *d-d* hybridization is stronger than for (3 Å)Au/(4.9 Å)Co/(10 Å)Au. One would have assumed here more Au neighbors per Co atom. However, the observed presence of the orbital moment anisotropy for (3 Å)Au/(4.9 Å)Co/(10 Å)Au indicates also the influence of a structural modification, which leads to a decrease in the strength of the Co-Au *d-d* hybridization. These results agree with the coexistence of in-plane and out-of-plane regions observed in the XMCD-PEEM data of Fig. 1, and support our assignment of the gray patches in Fig. 1(d) as areas with out-of-plane magnetization.

We now turn to the evolution of the remanent magnetization upon Au capping. With the deposition of just 3 Å of Au on the (4.9 Å)Co/(10 Å)Au structure the in-plane component of the effective spin moment at 100 K remains nearly constant at about 85% of its bulk value. The in-plane remanence at 300 K, though, increases up to 35%. The addition of more Au should, in principle, lead to an increase of the dots' magnetocrystalline anisotropy.[28] An increase of the out-of-plane response at the expense of the in-plane one indicates that more out-of-plane domains oriented in one direction are formed. The existence of a nonsaturated stable out-of-plane

magnetization component at 100 K would also be consistent with a tendency of the out-of-plane component to break up in domains with alternating "up-down" orientations. A strong magnetocrystalline anisotropy favors a single domain state in thin films. Thus the low values obtained here must be assigned to the relaxation of the remanence magnetization through the formation of "plus-minus" domains, as the strength of the coercive field should still remain below the applied field. In this context we note that for a couple of Co monolayers in Au/Co/Au sandwiches a coercive field of less than 1 kG was measured.[29] Due to the reduced lateral dimensions of our dots, a better guidance may be derived from another work in which Co nanopillars were grown on reconstructed Au surfaces.[30] Based on these results we expect the coercive field to be much smaller than 1 kG, allowing us to magnetically saturate the sample.

With further deposition of Au, no stable macroscopic out-of-plane remanence could be stabilized even at 100 K and the in-plane component at 300 and 100 K was greatly reduced. Such a result is clearly unexpected for continuous films, and it appears to be specific to the existence of Co entities on the surface. This behavior can be tentatively explained in terms of structural relaxation effects causing a decrease of the magnetocrystalline anisotropy or the effective magnetic dot volume, which would lead to a relative increase of thermal fluctuations. As a summary of this section, the present set of data provides a characterization of the spin reorientation transition for a regular array of (Au/Co/Au) nanodots; this appears to be much closer to the case of (Co/Au) monolayers on Au(111) single crystal[12] than to the (Au/Co/Au) trilayers grown on sapphire.[31]

Next, we will discuss the variation of the ratio of orbital-to-spin moment, which is displayed in Fig. 3(b). As mentioned above, this ratio is independent of the magnetic remanence value. Any strong changes of this ratio, as those observed in Fig. 3, can thus be understood as the result of variations of the orbital moment. The spin moment is expected to vary much less, of the order of 10% or less of its value.[32] This has indeed been found in previous studies for this system, both for Co monolayers on Au and as a function of Co thickness in capped (Au/Co/Au) trilayers.[24,27,28] From Fig. 3(b) it can be seen that the in-plane and out-of-plane data points at 100 K (squares) and the in-plane ones at 300 K (open circles) follow initially a roughly linear trend versus total Co and Au thickness. The initial slope, as defined by the second Co evaporation step for the (4.9 Å)Co/(10 Å)Au sample, is the same for in and out of plane at 100 K, and much higher than for in plane at 300 K. The increase of the ratio in a thickness range in which the spin moment is also increasing, as demonstrated in Fig. 3(a), implies an even stronger growth of the orbital moment. This reveals not only the importance of real-space structure effects in favoring a stable out-of-plane remanence as the overall thickness increases, but also the likely existence of a structure-related distortion, lowering the local crystal symmetry and leading to an increased anisotropy of the orbital moment as the magnetization rotates from in plane to out of plane.

The data for the two first Co evaporation steps measured at 100 K show the existence of a spin reorientation transition without an associated variation of the orbital moment, a fact that seems to contradict earlier calculations.[17] Our data indicate that, for a spin reorientation taking place in (Co/Au), it appears of more fundamental importance to induce a structural distortion in the lattice, mirrored in an overall increased value of the orbital moment.

The orbital-to-spin moment ratio for the in-plane data points at 100 K (open squares) is increasing with the two first Co evaporation steps. Moreover the observed trend (increase) for the out-of-plane data (filled squares) at 100 K is stronger than for in-plane data at 300 K (open circles) before the first Au capping. Such an observation appears to be correlated with the variation of a macroscopic out-of-plane remanence and therefore highlights a modification of the magnetic anisotropy energy, directly responsible for this stronger slope and overall high value of the orbital moment. Overall we observe that the spin reorientation transition for an array of dots takes place over a much wider temperature range (more than 200 K) than for other Au/Co/Au thin films.[31] Also important is the fact that almost no change in the slope of the out-of-plane ratio can be seen as the previously discussed (4.9 Å)Co/(10 Å)Au sample is covered with another Au layer 3 Å thick [solid squares in Fig. 3(b)], whereas the slope for the in-plane data points at 100 K decreases. Finally, with further Au capping an anomaly is found in the variation of the orbital moment at 100 K. For the highest Au capping thickness studied (4.3 Å) no out-of-plane magnetization could be observed. On the other hand, a similar increase of the in-plane ratios is detected at both 100 and 300 K. It is not clear which type of structural changes can be responsible for this behavior. Only upon cooling the (Co/Au) and (Au/Co/Au) samples we observe variation of the orbital moment, indicating either that structural distortions may occur upon cooling, or some variation in the roughness of the Co/Au interface takes place. In summary, the data of Fig. 3 for the orbital moment highlight the importance of structural distortions for the occurrence of a stable, macroscopic out-of-plane remanence.

B. Co *K*-edge EXAFS

Given the anomalous increase of the orbital moment found on the (Au/Co/Au) dots with respect to thin films it is of importance to correlate this observation with possible structural variations occurring at the level of the first few neighbor shells of the Co atoms. An increase of the orbital moment may be linked to structural distortions of the dots, lowering the local symmetry around the Co atoms, as compared to bulklike samples, but it may also be due to electronic structure effects. The latter are, in particular, related to the strong spin-orbit energy of the Au atoms. The information provided by Co *K*-edge EXAFS on the local environment of the Co atoms allows disentangling structural from electronic effects.

The EXAFS data were taken at room temperature for the (4.3 Å)Au/(4.9 Å)Co/(10 Å)Au sample and compared with the direct x-ray transmission from a Co foil, which was used as the reference sample.

The *k*-weighted EXAFS spectra of both samples are shown together after atomic background subtraction and nor-

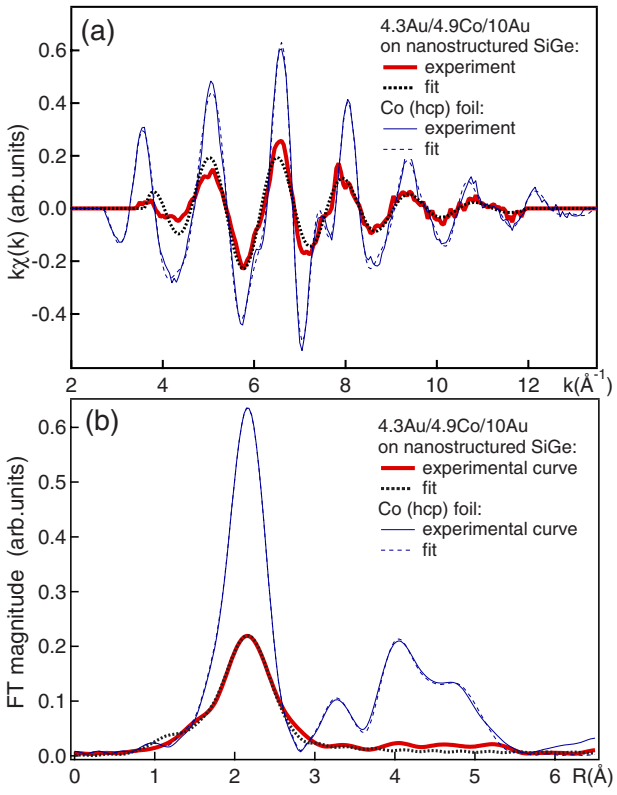

FIG. 4. (Color online) (a) Raw EXAFS oscillations of (4.3 Å)Au/(4.9 Å)Co/(10 Å)Au nanostructures grown on a self-organized $Si_{0.5}Ge_{0.5}$ substrate (thick solid line) and of a Co (hcp) foil (thin line) recorded at 12° grazing incidence of the x-ray beam at 300 K. For comparison the FEFF6 calculations of the nanostructured sample for the first two shells in the range 1.24 Å$<R<$3.20 Å and for the Co (hcp) foil performed in the range 1.24 Å$<R<$5.60 Å are presented at the same plot. (b) Fourier transform of $k\chi(k)$ of the EXAFS spectra of the nanostructured sample (thick solid line) and FT of Co (hcp) foil at 300 K are shown for comparison (thin line). Both best fits to the experimental results (a) and (b) (dashed lines) are shown together with the experimental results (solid lines).

malization to the atomic cross section of the K-absorption edge using the "Athena" software as thick and thin line in Fig. 4(a). The threshold energy E_0 was taken at the first inflection point at the value of 7709 eV for all the spectra. The data were then converted into photoelectron wave vector k space. To obtain the Fourier transform (FT) of the EXAFS signal in R space for the Co foil we used a k range from 2.7 to 13.4 Å^{-1}, whereas for the nanostructured sample we used a k range from 3.4 to 11.9 Å^{-1}. The FT of the EXAFS spectra for the (Au/Co/Au) dots and for the Co foil were calculated using the "Athena" and "Artemis" software and are shown in Fig. 4(b) as a thick and thin line, respectively. No phase shift correction was included in the FT data of Fig. 4(b).

For the (Au/Co/Au) dots, the atomic distances within the first two nearest neighbor shells contributing to the Fourier peak around 2 Å in Fig. 4(b) were calculated using a back Fourier transform of the first peak of the FT using the range 1.24 Å$<R<$3.20 Å. Here only single scattering is important. The FT of the standard Co foil shown in Fig. 4(b) (thin line) reproduces well the results from the literature[33,34] for Co with hcp stacking for both the distance and amplitude of the two first neighbor shells contributing to the main peak. In contrast, the atomic distances for the Co foil were calculated in a range of R: 1.24 Å$<R<$5.60 Å also accounting for the contribution of more distant neighbor shells and the multiple-scattering contributions within this distance range. The simulations were performed using the back filtered oscillations and the FEFF6 code from Artemis software.[23] The results of the best fit for the nanostructured sample and the Co hcp foil are shown in Fig. 4(b) as dashed lines with respect to each sample. The inelastic loss factor, S_0^2 parameter, was obtained by fitting the Co foil EXAFS for the nearest neighbor shells within the first peak and was 0.78. The S_0^2 factor was fixed for the dots to the same value. The E_0, the effective coordination number N^*, the distances of the two close lying nearest neighbor Co-Co shells R_1 and R_2, and mean-square relative-displacement factor σ^2, were determined by the Artemis fits. The E_0 value was found 6.0 ± 0.5 eV for both the Co foil and the dots. The results of the fits are presented in Table I.

TABLE I. Summary of the results of the EXAFS analysis using the FEFF6 code for the first two neighbor shells of Co. N^* is the effective coordination number, R is the first nearest neighbor distance, and σ^2 is a mean-square relative displacement factor. For the (Au/Co/Au) dots, a strong decrease of N^* is observed, and the first two Co shells are 0.12 Å apart.

Sample	N^* (±1)	R (Å^2)	σ^2 (Å^2)
Co foil	6	2.49 ± 0.01	0.0030 ± 0.0005
	6	2.51 ± 0.01	
Au/Co/Au	4	2.47 ± 0.02	0.0050 ± 0.0005
dots	3	2.59 ± 0.02	

Despite the fact that two close distances in the forward Fourier transformed (FFT) oscillations corresponding to the first peak are not completely resolved by the EXAFS experiment, the first peak can be fitted using the single scattering formalism with two close shells of 2.49 and 2.51 Å each comprising six neighbors with a mean-square relative displacement factor (σ^2) of 0.003 Å^2. The other peaks include single- and multiple-scattering contributions.

For the (Au/Co/Au) dots (thick lines in Fig. 4) we find a strong reduction of the EXAFS amplitude for all peaks with respect to the Co (hcp) foil. The best EXAFS fit indicates a loss of about 5 of the Co neighbors within the first peak of the FT. The effective coordination number N^* was calculated only for Co neighbors neglecting the Au nearest neighbor contributions.

All attempts to include Au neighbors considerably deteriorated the quality of the fit in agreement with the results for Au/Co/Au multilayers[34] and Co on Au(111).[33] These studies already indicate that in the EXAFS signal the Au atoms are not making a contribution due to the increased disorder of the Co-Au bonds. The strong reduction in coordination number confirms the fact that only a couple of Co monolayers are embedded in Au. The data analysis and FEFF calcu-

lations give the best fit to the back-filtered EXAFS oscillations for the first peak of the FT, with two distinct Co shells around 2.5 and 2.6 Å, respectively. These values are both smaller than 2.88 Å, indicating a nonpseudomorphic growth of Co on the Au underlayer in contrast to what has been found by EXAFS for (Co/Au) multilayers.[34]

It must be kept in mind that the Au underlayer is deposited directly onto amorphous native oxide existing on the semiconductor substrate surface.[9] We thus expect that this Au underlayer will be polycrystalline with (111) texture, since this is the face with the lowest energy, and our results can be compared with previous work on layered systems.[35] Such a model is in agreement with the observation of the occurrence of the spin reorientation (SR) at the specific Co thickness for our dots, similar as for Co/Au(111).[12] The specific thickness for the appearance of the SR is strongly influenced by the Co crystallographic structure.[26] Indeed a similar Co-Co nearest neighbor distance coupled with a nonpseudomorphic growth was found for Co/Au(111).[33]

In the case of Co monolayers on a single Au(111) crystal the first Co-Co distance was determined as 2.51 Å.[33] We observe, however, the existence of two distinct Co shells in the case of our dots. The EXAFS results, obtained after Au capping [data point (4.3 Å)Au/(4.9 Å)Co/(10 Å)Au in Fig. 3(b)] indicate the existence of considerable strain in the Co lattice. The sudden increase of in-plane orbital moment upon increasing the Au capping to reach 4.3 Å suggests the occurrence of a structural relaxation releasing partly the Co lattice epitaxial strain. This observation leads to the assumption of even higher strain in the Co lattice, correlating with the out-of-plane magnetization at lower layer thickness shown in Fig. 3.

First-principle calculations for a Co monolayer embedded in Au report that *s*, *p-d* hybridization at the interface leads to orbital moment anisotropy ($m_{\text{in plane}}$-$m_{\text{out of plane}}$) of $0.08\mu_B$.[36] Experiments have demonstrated even higher values for the orbital moment anisotropy, correlating with the occurrence of out-of-plane magnetization.[24,25] The data of Fig. 3(b) indicate however, surprisingly, that it is possible to obtain an out-of-plane magnetic moment also with a very weak in-versus out-of-plane anisotropy of the orbital moment [data point for (4.9 Å)Co/(10 Å)Au in Fig. 3(b)]. At the same time only a bulklike value of $0.14\mu_B$ is found for the orbital moment. The EXAFS analysis thus highlights the importance of the magnetoelastic contribution to the magnetic anisotropy energy in this context.

IV. CONCLUSION

We have demonstrated the existence of stable remanence in arrays of self-organized (Co/Au) and (Au/Co/Au) magnetic nanodots grown on nanostructured self-organized SiGe substrates. In-plane magnetic order, favored by the magnetostatic coupling between dots, becomes stable even at room temperature for nearly all Co thicknesses. On the contrary, the well-known perpendicular anisotropy characteristic of (Co/Au) multilayers is reduced in these low-dimensional islands, in such a way that out-of-plane magnetization can only be stabilized at low temperature (100 K), and is correlated with an increase of the orbital magnetic moment. Our structural and magnetic characterization of the spin reorientation transition in these nanomagnet arrays by means of XPEEM, EXAFS, and XMCD measurements reveals several interesting features. It takes place over a much broader thickness range than in two-dimensional multilayers, and is not necessarily accompanied by a variation in the orbital moment as previously expected. Significant structural relaxations have been detected in the Co that probably play a major role in determining the magnetic behavior of these dot arrays.

ACKNOWLEDGMENTS

We want to thank the staff of the Elettra and MAX-lab synchrotrons for their assistance with the realization of these experiments. We further thank M. Oehme, K. Lyutovich, and E. Kasper, University of Stuttgart, for growing the SiGe samples. This work has been supported by the EC STReP NAMASOS Project (Grant No. STRP NMP 505854), the Swedish Research Council, and the Göran Gustafsson Foundation. Work by the Spanish group was also partially supported by Grants No. FIS2007-61114, No. NANOMAGNET S-0505/MAT/0194, and Consolider Molecular Science.

*Corresponding author; present address: MAX-lab, Box 118, S-22100, Lund, Sweden.

†Present address: Sincrotrone Trieste, S.S. 14, km 163.5, 34012 Basovizza, Trieste, Italy.

[1] G. E. Moore, Electronics Magazine **38**(8) (1965). See, also, http://en.wikipedia.org/wiki/Moore%27s_law

[2] B. D. Terris and T. Thomson, J. Phys. D **38**, R199 (2005).

[3] V. Skumryev, S. Stoyanov, Y. Zhang, G. Hadjipanayis, D. Givord, and J. Nogués, Nature (London) **423**, 850 (2003).

[4] S. I. Kiselev, J. C. Sankey, I. N. Krivorotov, N. C. Emley, R. J. Schoelkopf, R. A. Buhrman, and D. C. Ralph, Nature (London) **425**, 380 (2003).

[5] A. Moser, K. Takano, D. T. Margulies, M. Albrecht, Y. Sonobe, Y. Ikeda, S. Sun, and E. E. Fullerton, J. Phys. D **35**, R157 (2002).

[6] L. Néel, J. Phys. Radium **15**, 225 (1954).

[7] H. Haken, *Synergetics. An Introduction: Non-Equilibrium Phase Transitions and Self-Organisation in Physics, Chemistry and Biology*, 3rd ed. (Springer, Berlin, 1983).

[8] C. Teichert, Appl. Phys. A: Mater. Sci. Process. **76**, 653 (2003).

[9] C. Teichert, Phys. Rep. **365**, 335 (2002).

[10] C. Teichert, J. Barthel, H. P. Oepen, and J. Kirschner, Appl. Phys. Lett. **74**, 588 (1999).

[11] A. M. Mulders, A. F. Rodríguez, D. Arvanitis, C. Hofer, C. Teichert, M. Á. Niño, J. Camarero, J. J. de Miguel, R. Miranda, K. Lyutovich, E. Kasper, S. Heun, and A. Locatelli, Phys. Rev. B **71**, 214422 (2005).

[12] R. Allenspach, M. Stampanoni, and A. Bischof, Phys. Rev. Lett. **65**, 3344 (1990).
[13] R. P. Cowburn, D. K. Koltsov, A. O. Adeyeye, M. E. Welland, and D. M. Tricker, Phys. Rev. Lett. **83**, 1042 (1999).
[14] L. Giovannini, F. Montoncello, F. Nizzoli, G. Gubbiotti, G. Carlotti, T. Okuno, T. Shinjo, and M. Grimsditch, Phys. Rev. B **70**, 172404 (2004).
[15] C. Hofer, C. Teichert, M. Wächter, T. Bobek, K. Lyutovich, and E. Kasper, Superlattices Microstruct. **36**, 281 (2004).
[16] P. Carra, B. T. Thole, M. Altarelli, and X. Wang, Phys. Rev. Lett. **70**, 694 (1993).
[17] P. Bruno, Phys. Rev. B **39**, 865 (1989).
[18] D. Arvanitis, M. Tischer, J. Hunter-Dunn, F. May, N. Mårtensson, and K. Baberschke, *Experimental Determination of Orbital and Spin Moments from MCXD on 3D Metal Overlayers*, in Proceedings of the workshop "Spin influenced Spectroscopies of Magnetic Solids," edited by H. Ebert and G. Schuetz, Lecture Notes in Physics Vol. 466 (Springer-Verlag, Berlin, 1996), ISBN 3-540-60843-5.
[19] http://www.maxlab.lu.se/beamlines/bld1011/
[20] J. Hunter-Dunn, A. Hahlin, O. Karis, D. Arvanitis, G. LeBlanc, Å. Andersson, and L.-J. Lindgren, *Eighth International Conference on Synchrotron Radiation Instrumentation*, AIP Conf. Proc. No. 705 (AIP, Melville, NY, 2004), p. 65.
[21] J. Langer, J. H. Dunn, A. Hahlin, O. Karis, R. Sellmann, D. Arvanitis, and H. Maletta, Phys. Rev. B **66**, 172401 (2002).
[22] S. Carlsson, M. Clausén, L. Gridneva, B. Sommarin, and C. Svensson, J. Synchrotron Radiat. **13**, 359 (2006).
[23] B. Ravel and M. Newville, J. Synchrotron Radiat. **12**, 537 (2005).
[24] T. Koide, H. Miyauchi, J. Okamoto, T. Shidara, A. Fujimori, H. Fukutani, K. Amemiya, H. Takeshita, S. Yuasa, T. Katayama, and Y. Suzuki, Phys. Rev. Lett. **87**, 257201 (2001).
[25] J. Stöhr, J. Magn. Magn. Mater. **200**, 470 (1999).
[26] C. Andersson, B. Sanyal, O. Eriksson, L. Nordström, O. Karis, D. Arvanitis, T. Konishi, E. Holub-Krappe, and J. H. Dunn, Phys. Rev. Lett. **99**, 177207 (2007).
[27] C. Andersson, Ph.D. thesis, Uppsala University, 2006, ISBN-91-554-6554-4, http://publications.uu.se/
[28] D. Weller, J. Stöhr, R. Nakajima, A. Carl, M. G. Samant, C. Chappert, R. Megy, P. Beauvillain, P. Veillet, and G. A. Held, Phys. Rev. Lett. **75**, 3752 (1995).
[29] B. N. Engel, C. Marlière, and C. M. Falco, IEEE Trans. Magn. **31**, 4080 (1995).
[30] O. Fruchart, P.-O. Jubert, C. Meyer, M. Klaua, J. Barthel, and J. Kirschner, J. Magn. Magn. Mater. **239**, 224 (2002).
[31] R. Sellmann, H. Fritzsche, H. Maletta, V. Leiner, and R. Siebrecht, Phys. Rev. B **64**, 054418 (2001).
[32] O. Hjortstam, J. Trygg, J. M. Wills, B. Johansson, and O. Eriksson, Phys. Rev. B **53**, 9204 (1996).
[33] N. Marsot, R. Belkhou, H. Magnan, P. Le Fevre, C. Guillot, and D. Chandesris, Phys. Rev. B **59**, 3135 (1999).
[34] S. Pizzini, F. Baudelet, E. Dartyge, A. Fontaine, Ch. Giorgetti, J. F. Bobo, M. Piecuch, and C. Marlière, J. Magn. Magn. Mater. **121**, 208 (1993).
[35] M. J. Rost, D. A. Quist, and J. W. M. Frenken, Phys. Rev. Lett. **91**, 026101 (2003).
[36] B. Újfalussy, L. Szunyogh, P. Bruno, and P. Weinberger, Phys. Rev. Lett. **77**, 1805 (1996).